Structural Engineering and Mechanics, Vol. 34, No. 6 (2010) 703-718
DOI: http://dx.doi.org/10.12989/sem.2010.34.6.703

The use of discontinuous first and second-order mixed boundary elements for 2D elastostatics

M.H. Severcan[1*], A.K. Tanrikulu[2], A.H. Tanrikulu[2] and I.O. Deneme[3]

[1]*Department of Civil Engineering, Nigde University, 51100 Merkez, Nigde, Turkey*
[2]*Department of Civil Engineering, Cukurova University, 01330 Balcali, Adana, Turkey*
[3]*Department of Civil Engineering, Aksaray University, 68100 Merkez, Aksaray, Turkey*

(Received September 1, 2008, Accepted December 24, 2009)

Abstract. In classical higher-order discontinuous boundary element formulation for two-dimensional elastostatics, interpolation functions for different boundary variables (i.e., boundary displacements and tractions) are assumed to be the same. However, there is a derivational relationship between these variables. This paper presents a boundary element formulation, called *Mixed Boundary Element Formulation*, for two dimensional elastostatic problems in which above mentioned relationship is taking into account. The formulations are performed by using discontinuous first and second-order mixed boundary elements. Based on the formulations presented in this study, two computer softwares are developed and verified through some example problems. The results show that the present formulation is credible.

Keywords: boundary element method; discontinuous mixed boundary element; two dimensional elastostatics.

1. Introduction

As is well known, the boundary element method (BEM) in elasticity is based on displacement boundary integral equation formulations of boundary value problems. The BEM has been applied quite successfully to two dimensional elastostatic problems (Brebbia and Dominguez 1989, Banerjee 1994).

The BEM employing discontinuous higher-order elements where the nodes are all placed internally offers the advantage of high accuracy for two dimensional elastostatic problems (Dyka and Millwater 1989, Zhang and Zhang 2003). Also, the discontinuous boundary elements have advantages of effectively tackling the corner nodes effect, discontinuous traction etc. (Zhang and Zhang 2003).

In classical higher-order discontinuous boundary element formulation for two-dimensional elastostatics, interpolation functions for different boundary variables (i.e., boundary displacements and tractions) are assumed to be the same. However, there is a derivational relationship between these variables. This paper presents a boundary element formulation, called *Mixed Boundary*

*Corresponding author, Ph.D., E-mail: msever@nigde.edu.tr

Element Formulation, for two dimensional elastostatic problems in which above mentioned relationship is taking into account. In the formulation first-order and second-order mixed boundary elements are used.

In the first-order discontinuous mixed boundary element formulation, the boundary of the two dimensional domain is divided into several linear boundary elements having two nodes. It is assumed that, variation of the displacement is linear whereas the traction is constant over the elements. This assumption is based on the fact that the traction on a boundary is space derivative of the displacement of that boundary. Similarly, in the second-order discontinuous mixed boundary element formulation, the boundary of the two dimensional domain is divided into several quadratic elements having three nodes, variation of the displacement is taken as quadratic and the traction is assumed to be linear over the elements. Thus, without reducing the accuracy of the solution is aimed to reduce the total number of unknowns and the computing time of the solution.

In contrast to other discretization methods, the Boundary Element Methods involve the nearly singular integrals. Nearly singular integrals are occurred when the source point is close to the field point. Evaluation of the nearly singular integrals is not a simple task. There are several techniques available in literature to evaluate the nearly singular integrals (Liu *et al.* 1993, Sladek and Sladek 1998, Sladek *et al.* 2001).

In this paper, depending on the order of the formulation, the nearly singular integrals are evaluated by semi-analytical or numerical techniques which are both discussed in the third section in detail.

Based on the formulation, two computer softwares, namely, BEMLC and BEMQL (for discontinuous first and second-order mixed boundary element formulation respectively) are developed for solving two-dimensional problems in elastostatics. The softwares have been verified through the analysis of sample problems.

The classical boundary element formulation for two-dimensional elastostatics is well established in literature (Brebbia and Dominguez 1989, Banerjee 1994, Manolis and Beskos 1987, Mengi *et al.* 1994). For the sake of completeness, some basic equations of the formulation are presented below.

2. Boundary element equation for two dimensional elastostatics

In the absence of body forces, the boundary element equation for two-dimensional elastic domain can be written as

$$c_{\ell i}u_i(A) = \int_S G_{\ell i}(A,P)t_i(P)dS - \int_S H_{\ell i}(A,P)u_i(P)dS \tag{1}$$

Here, A and P are source (fixed) and field (integration) points respectively (see Fig. 1), u_i and t_i are displacement and traction components of the points A and P respectively. $c_{\ell i}$ is a constant depending on the location of A. $G_{\ell i}$ and $H_{\ell i}$ represent first and second fundamental solutions. In writing Eq. (1), the indicial notation is used, and it is assumed that the indices appearing in this equation have the range from 1 to 2. Repeated index implies summation over the range of that index.

Boundary element equation, Eq. (1), can be rewritten in matrix form as

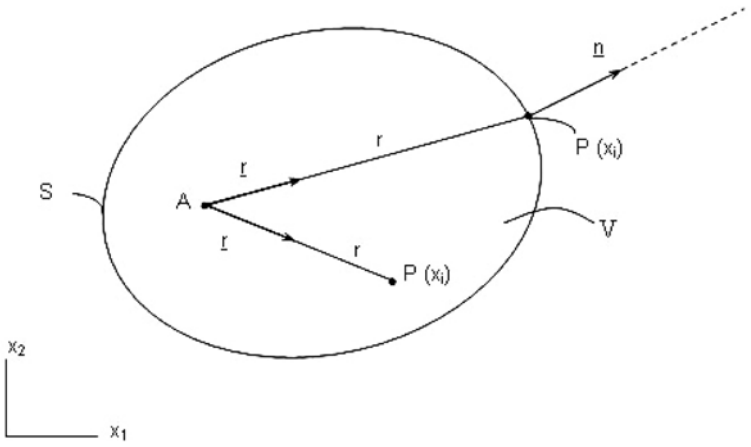

Fig. 1 A two dimensional elastic domain

$$\mathbf{cu}(A) = \int_S \mathbf{G}(A,P)\mathbf{t}(P)dS - \int_S \mathbf{H}(A,P)\mathbf{u}(P)dS \tag{2}$$

In Eq. (2), **c** is a matrix which is

$$\mathbf{c} = \begin{cases} \mathbf{I}, \text{ if } A \text{ is an interior point} \\ \mathbf{0}, \text{ if } A \text{ is outside of the domain } V \\ \tfrac{1}{2}\,\mathbf{I}, \text{ if } A \text{ is on the boundary } S \end{cases}$$

where **I** is identity matrix. It may be noted that the last expression above does not hold when A is a corner point (Brebbia and Dominguez 1989). The fundamental solutions **G** and **H** of elastostatics have been presented in literature by taking the auxiliary system as infinite (Mengi *et al.* 1994). The unknown displacement and traction components (*boundary quantities*) on the boundary S can be determined by solving the boundary element equation together with boundary conditions.

3. Numerical solution of boundary element equation

The boundary element equation can be solved numerically by discretizing the boundary S into small discontinuous boundary elements (see Fig. 2) and using some shape functions for the approximation of the distribution of boundary quantities over the elements.

3.1 Discontinuous first-order mixed boundary element formulation

In the discontinuous first-order mixed boundary element formulation, it is assumed that the variations of the displacements are linear and stresses are constant over the element.

For the numerical solution, the boundary is discretized into N discontinuous linear boundary elements and two nodal points are placed within the elements (see Fig. 3).

When the boundary element equation, Eq. (2), is written at the kth node of the mth boundary element (P_m^k, k = 1, 2), in view of discontinuous first-order mixed element formulation, one gets

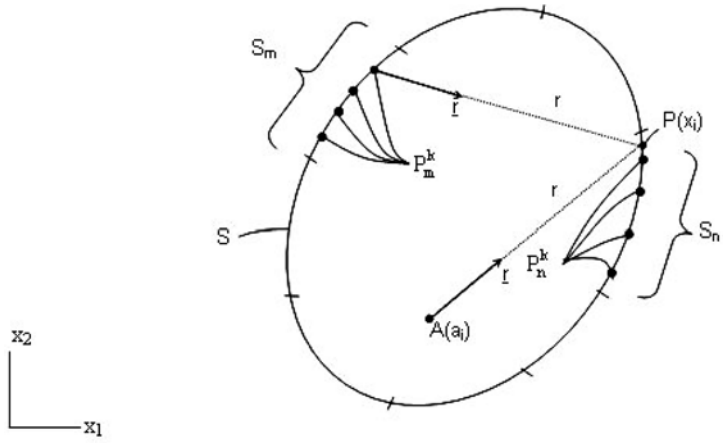

Fig. 2 Boundary element discretization of the body

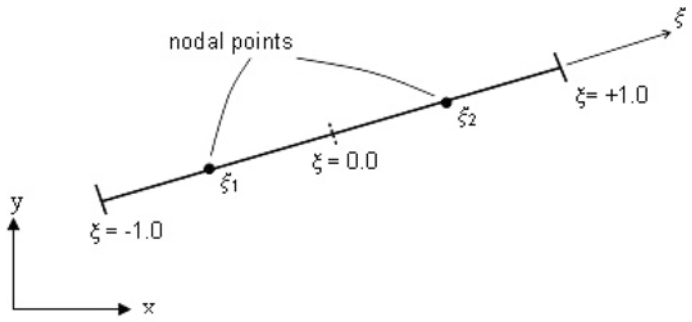

Fig. 3 A typical discontinuous linear boundary element

$$\frac{1}{2}\mathbf{I}\mathbf{u}(P_m^k) = \sum_{n=1}^{N}\int_{S_n}\mathbf{G}(P_m^k, P)\mathbf{t}(P)dS - \sum_{n=1}^{N}\int_{S_n}\mathbf{H}(P_m^k, P)\mathbf{u}(P)dS \tag{3}$$

It should be noted that, in the discontinuous element approach, the node P_m^k is not a corner point. Thus, in writing Eq. (3), $\mathbf{c} = \frac{1}{2}\mathbf{I}$ is used.

According to the discontinuous first-order mixed element formulation, coordinates of a point on the boundary element and its displacement and traction components can be defined as

$$x_i = \sum_{k=1}^{2}\phi_k(\xi)x_i^k \tag{4}$$

$$u_i = \sum_{k=1}^{2}\phi_k(\xi)u_i^k \tag{5}$$

$$t_i = \sum_{k=1}^{2}\psi_k(\xi)t_i^k \tag{6}$$

where x_i^k, u_i^k and t_i^k (k = 1, 2) denote the global coordinates, displacements and stresses of the nodal points respectively, ξ is the natural coordinate of the point, $\phi_k s$ (k = 1, 2) are the linear shape functions which are given in the natural coordinates by

$$\phi_1(\xi) = \left(\frac{\xi_2 - \xi}{\xi_2 - \xi_1}\right), \quad \phi_2(\xi) = \left(\frac{\xi - \xi_1}{\xi_2 - \xi_1}\right), \quad -1 < \xi_1 < 0\,,\ 0 < \xi_2 < 1 \tag{7}$$

where ξ_1 and ξ_2 are the natural coordinates of first and second nodal points respectively, and the stress interpolation functions $\psi_k s$ are selected as

$$\psi_1 = 1\,, \quad \psi_2 = 0 \tag{8}$$

Thus, the stress values over the element are taken as constant and equal to the stress values at the first nodal point of that element.

Using Eqs. (5) and (6), Eq. (3) can be rewritten as

$$\frac{1}{2}\mathbf{I}\mathbf{u}(P_m^k) = \sum_{n=1}^{N}\sum_{s=1}^{2}\left[\int_{-1}^{1} J\mathbf{G}(P_m^k, P)\psi_s d\xi\right]\mathbf{t}(P_n^s) - \sum_{n=1}^{N}\sum_{s=1}^{2}\left[\int_{-1}^{1} J\mathbf{H}(P_m^k, P)\varphi_s d\xi\right]\mathbf{u}(P_n^s) \tag{9}$$

where $\mathbf{t}(P_n^s)$ and $\mathbf{u}(P_n^s)$ denote the traction and displacement vectors at sth nodal point of the nth element, respectively. It should be noted that, the integration parameter dS in Eq. (3) is transformed as

$$dS = Jd\xi = \sqrt{\left[\frac{dx_1(\xi)}{d\xi}\right]^2 + \left[\frac{dx_2(\xi)}{d\xi}\right]^2}\, d\xi \tag{10}$$

where J is the Jacobian. Since the linear element assumption, here, the Jacobian is constant and equals to half of the element length. The shape function matrices ($\boldsymbol{\phi}_s$, $\boldsymbol{\psi}_s$) in Eq. (9) are

$$\boldsymbol{\varphi}_s = \begin{bmatrix} \phi_s & 0 \\ 0 & \phi_s \end{bmatrix}; \quad \boldsymbol{\psi}_s = \begin{bmatrix} \psi_s & 0 \\ 0 & \psi_s \end{bmatrix} \quad (s = 1, 2) \tag{11}$$

If the following definitions are made

$$\mathbf{G}_{ks}^{mn} = \int_{-1}^{1} J\mathbf{G}(P_m^k, P)\psi_s d\xi, \quad \mathbf{H}_{ks}^{mn} = \int_{-1}^{1} J\mathbf{H}(P_m^k, P)\varphi_s d\xi \tag{12}$$

Eq. (9) can be rewritten as

$$\frac{1}{2}\mathbf{I}\mathbf{u}(P_m^k) = \sum_{n=1}^{N}\sum_{s=1}^{2}\mathbf{G}_{ks}^{mn}\mathbf{t}(P_n^s) - \sum_{n=1}^{N}\sum_{s=1}^{2}\mathbf{H}_{ks}^{mn}\mathbf{u}(P_n^s) \tag{13}$$

When Eq. (13) is written for the source points P_m^k (k = 1, 2) of the mth element and combined, the following expression is obtained

$$\mathbf{c}^m\mathbf{u}^m = \sum_{n=1}^{N}\mathbf{G}^{mn}\mathbf{t}^n - \sum_{n=1}^{N}\mathbf{H}^{mn}\mathbf{u}^n \tag{14}$$

where the matrix and vectors are

$$\mathbf{G}^{mn}=\begin{bmatrix}\mathbf{G}_{11}^{mn} & \mathbf{G}_{12}^{mn}\\ \mathbf{G}_{21}^{mn} & \mathbf{G}_{22}^{mn}\end{bmatrix},\quad \mathbf{H}^{mn}=\begin{bmatrix}\mathbf{H}_{11}^{mn} & \mathbf{H}_{12}^{mn}\\ \mathbf{H}_{21}^{mn} & \mathbf{H}_{22}^{mn}\end{bmatrix}$$
$$\mathbf{u}^{n}=\begin{bmatrix}\mathbf{u}(P_n^1)\\ \mathbf{u}(P_n^2)\end{bmatrix},\quad \mathbf{t}^{n}=\begin{bmatrix}\mathbf{t}(P_n^1)\\ \mathbf{t}(P_n^2)\end{bmatrix},\quad \mathbf{c}^{m}=\begin{bmatrix}\frac{1}{2}\mathbf{I} & \mathbf{0}\\ \mathbf{0} & \frac{1}{2}\mathbf{I}\end{bmatrix} \tag{15}$$

After the Eq. (14) is written for all boundary elements ($m = 1, \ldots, N$) and combined, the system equations of BEM can be obtained in matrix form

$$\tilde{\mathbf{H}}\tilde{\mathbf{u}} = \tilde{\mathbf{G}}\tilde{\mathbf{t}} \tag{16}$$

where

$$\tilde{\mathbf{G}} = (\mathbf{G}^{mn});\quad \tilde{\mathbf{H}} = \left(\mathbf{H}^{mn}+\frac{1}{2}\mathbf{I}\delta_{mn}\right);\quad \tilde{\mathbf{u}} = (\mathbf{u}^{n});\quad \tilde{\mathbf{t}} = (\mathbf{t}^{n})\quad (m,n=1,2,\ldots,N) \tag{17}$$

with δ_{mn} is Kronecker's delta. The elements $\mathbf{G}^{mn}$ and $\mathbf{H}^{mn}$ may be computed numerically by using Gaussian Quadrature Formula.

The solution of Eq. (16), together with the prescribed boundary conditions, determines numerically the unknown boundary quantities. Having determined unknown boundary quantities, if desired, the interior displacements and stresses can be computed numerically using the boundary quantities (Mengi *et al.* 1994).

Calculation of singular integrals

The matrices $\mathbf{G}_{ks}^{mm}$ and $\mathbf{H}_{ks}^{mm}$ which appear on the diagonals of the system matrices $\tilde{\mathbf{G}}$ and $\tilde{\mathbf{H}}$ in Eq. (16) are written as

$$\mathbf{G}_{ks}^{mm} = \int_{S_m}\mathbf{G}(P_m^k,P)\psi_s dS;\quad \mathbf{H}_{ks}^{mm} = \int_{S_m}\mathbf{H}(P_m^k,P)\varphi_s dS \tag{18}$$

where k denotes the number of the source point, and s indicates the shape function's number ($k, s = 1, 2$).

In these equations, source nodal point P_m^k and field point P are on the same element S_m. We note that Eqs. (18) are defined in the sense of Cauchy principle value, that is, S_m in Eqs. (18) does not include the source point P_m^k. Even so, since the points P_m^k and P are on the same element, in the case of $k = s$ the distance r between them might become very small, which makes the integrals in Eqs. (18) nearly singular (see Fig. 4).

For the first fundamental solution case, the singular integral is divided into two integral which contain $\ln(1/r)$ and $(1/r)$ singularities. Hence, the first fundamental solution is written as

$$G_{\ell i}^{kk} = A\left[\int_{-1}^{1}BJ\psi_k\ln(1/r)\delta_{\ell i}d\xi+\int_{-1}^{1}J\psi_k\left(\frac{x_\ell(\xi)-a_\ell}{r}\right)\left(\frac{x_i(\xi)-a_i}{r}\right)d\xi\right] \tag{19}$$

where $x_\ell(\xi)$ and $x_i(\xi)$ (ℓ, $i = 1$, 2) denote the coordinates of field point; a_ℓ and a_i indicate the

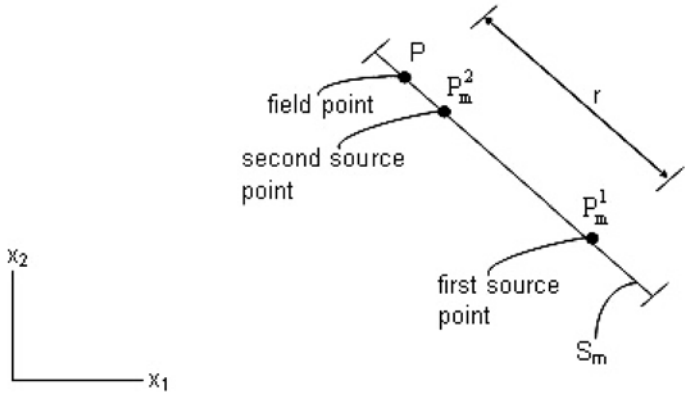

Fig. 4 Singular element

coordinates of the source point, A and B are material constants defined as follows

$$A = \frac{1}{8\pi\mu(1-\nu)}; \quad B = 3-4\nu \tag{20}$$

In the computation of $G_{\ell i}^{11}$, the integral with singularity $(1/r)$ in Eq. (19) is calculated numerically by using *Gaussian Quadrature*. For the calculation of the integral with singularity $\ln(1/r)$, the distance r (see Fig. 4) is redefined as

$$r = J|\xi + \xi_1| \tag{21}$$

where ξ_1 denotes the natural coordinate of the first source point (see Fig. 4). Hence, the integral with singularity $\ln(1/r)$ is calculated analytically by using following equation

$$\int_{-1}^{1} BJ\psi_1 \ln(1/r)\,\delta_{\ell i} d\xi = BJ\delta_{\ell i}\left[2 + (1-\xi_1)\ln\left(\frac{1}{J(1-\xi_1)}\right) + (1+\xi_1)\ln\left(\frac{1}{J(1+\xi_1)}\right)\right] \tag{22}$$

On the other hand, due to the second shape function ψ_2 is equal to zero, $G_{\ell i}^{22}$ becomes zero.

The elements of matrix $\mathbf{H}_{kk}^{mm}$, which include the second fundamental solution, can be obtained by means of the condition of rigid body movement as in Eq. (23) (Brebbia and Dominguez 1989).

$$\mathbf{H}_{kk}^{mm} = -\sum_{n=1}^{N}\sum_{s=1}^{2}\mathbf{H}_{ks}^{mn} \quad (\text{for } m \neq n \text{ and } k \neq s) \tag{23}$$

3.2 Discontinuous second-order mixed boundary element formulation

In discontinuous second-order mixed boundary element formulation we assume that the variation of the displacements and stresses over the element are quadratic and linear, respectively.

For the numerical solution, the boundary is discretized into N discontinuous quadratic boundary elements and three nodal points are placed within the elements (see Fig. 5).

In this case, coordinates of a point on the boundary element and its displacement and traction components can be defined in terms of the nodal values as

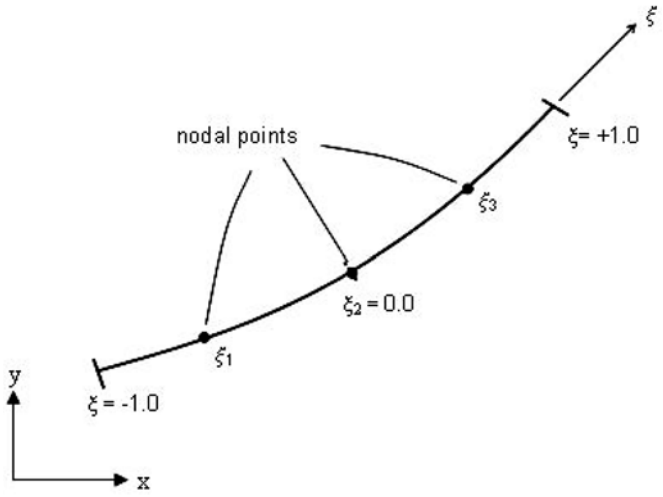

Fig. 5 A typical discontinuous quadratic boundary element

$$x_i = \sum_{k=1}^{3} \phi_k(\xi) x_i^k \tag{24}$$

$$u_i = \sum_{k=1}^{3} \phi_k(\xi) u_i^k \tag{25}$$

$$t_i = \sum_{k=1}^{3} \psi_k(\xi) t_i^k \tag{26}$$

Here, $\phi_k s$ (k = 1-3) are the quadratic shape functions which are given in the natural coordinates by

$$\phi_1(\xi) = \frac{\xi(\xi - \xi_3)}{\xi_1(\xi_1 - \xi_3)}, \quad \phi_2(\xi) = 1 - \frac{\xi(\xi_3 + \xi_1 - \xi)}{\xi_1 \xi_3}, \quad \phi_3(\xi) = \frac{\xi(\xi - \xi_1)}{\xi_3(\xi_3 - \xi_1)} \tag{27}$$

where ξ_1 $(-1 < \xi_1 < 0)$ and ξ_3 $(0 < \xi_3 < 1)$ are the natural coordinates of first and third nodal points, respectively, and the stress interpolation functions $\psi_k s$ are selected as

$$\psi_1(\xi) = \left(\frac{\xi_3 - \xi}{\xi_3 - \xi_1}\right); \quad \psi_2 = 0; \quad \psi_3(\xi) = \left(\frac{\xi - \xi_1}{\xi_3 - \xi_1}\right) \tag{28}$$

Thus, the variations of the stress values over the element are assumed to be linear in terms of first and third nodal values.

Using Eqs. (25) and (26), Eq. (3) can be rewritten as

$$\frac{1}{2}\mathbf{I}\mathbf{u}(P_m^k) = \sum_{n=1}^{N}\sum_{s=1}^{3}\left[\int_{-1}^{1} J(\xi)\mathbf{G}(P_m^k, P)\psi_s d\xi\right]\mathbf{t}(P_n^s) - \sum_{n=1}^{N}\sum_{s=1}^{3}\left[\int_{-1}^{1} J(\xi)\mathbf{H}(P_m^k, P)\varphi_s d\xi\right]\mathbf{u}(P_n^s) \tag{29}$$

where all the terms are defined as the same as Section 3.1. When the formulation steps similar in Section 3.1 are followed, similar system equation is obtained and solved for unknown boundary quantities. It should be noted that, in this case, the singular integrals existing in the first fundamental solution are calculated numerically by using *Gaussian Quadrature* (Becker 1992).

4. Numerical examples

In this section, some numerical examples are solved for the verification of the present formulation. To this end, based on the abovementioned formulation, two computer softwares have been developed, namely, BEMLC (for the discontinuous first-order mixed boundary element formulation) and BEMQL (for the discontinuous second-order mixed boundary element formulation).

Three examples are solved by using the softwares to demonstrate the suitability and accuracy of the present formulation comparing with the results obtained by analytically and using constant, discontinuous pure linear and discontinuous pure quadratic boundary element formulations in the literature.

In the analysis, the nodal locations of the discontinuous first-order mixed boundary elements are selected as $\xi_1 = -1/2$ and $\xi_2 = 1/2$ and the integrals are performed by using *ten-point* Gaussian Quadrature rule. The nodal locations of the discontinuous second-order mixed boundary elements are selected as $\xi_1 = -2/3$, $\xi_2 = 0$, $\xi_3 = 2/3$ and the integrals are fulfilled by using *six-point* Gaussian Quadrature rule.

4.1 Circular disk problem

This example considers a circular disk of radius a subjected to a uniaxial compressional force p as shown in Fig. 6(a). Except the points C and D where the force p is applied, the boundary of the disk is free of tractions. Symmetry conditions reduce the problem to the one shown in Fig. 6(b), where along the horizontal line AB the vertical displacement and horizontal traction vanish ($u_2 = t_1 = 0$ along AB). Here, the stress component τ_{22} along the horizontal line AB is investigated.

This plane stress problem is solved by using the software BEMLC and BEMQL. The analysis is carried out in nondimensional space. The nondimensional variables are defined as

$$\begin{gathered} \bar{x}_i = \frac{x_i}{d}; \quad \bar{u}_i = \frac{u_i}{d}; \quad \bar{t}_i = \frac{t_i}{\mu} \quad (i = 1, 2) \\ \bar{p} = \frac{p}{\mu d}; \quad \bar{\mu} = \frac{\mu}{\mu} = 1; \quad \bar{d} = \frac{d}{d} = 1 \end{gathered} \tag{30}$$

where $d = 2a$ is the diameter of the disk and μ is the shear modulus. In the analysis, Poisson's ratio and non-dimensional force are taken as $\nu = 0.25$ and $\bar{p} = 1$. Using symmetries, only one half of the disk is modeled using 40 and 15 elements for horizontal line AB and the circular line BCA, respectively as shown in Fig. 7. The vertical applied load acting at the point C is uniformly distributed over the element 48 of length 0.104 (see Fig. 7), which results in a traction value

$$\bar{t}_2 = -\frac{1}{0.104} = -9.62 \tag{31}$$

for that element.

The distribution of the stress component τ_{22} along the horizontal line AB obtained BEMLC and BEMQL is compared with the results obtained by constant BEM (BEMCC) (Mengi *et al.* 1994), discontinuous pure linear BEM (BEMLL) (Severcan 2004), discontinuous pure quadratic BEM (BEMQQ) (Severcan 2004) and the exact one in Fig. 8, where the non-dimensional $\bar{\tau}_{22}$ is defined by

$$\bar{\tau}_{22} = \frac{\tau_{22} d}{p} \tag{32}$$

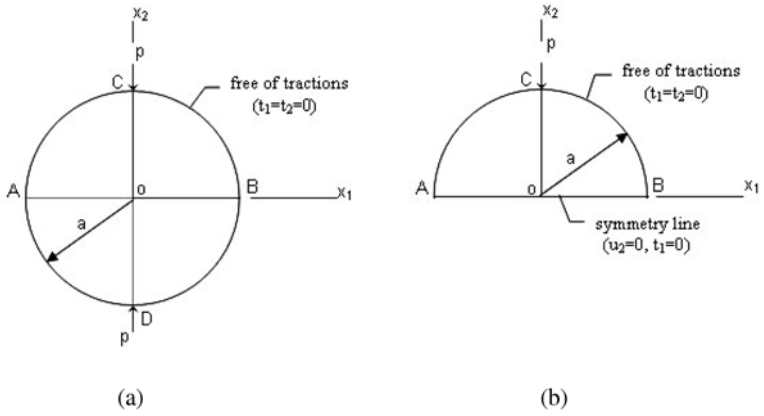

Fig. 6 Circular disk subjected to a uniaxial compressional force p

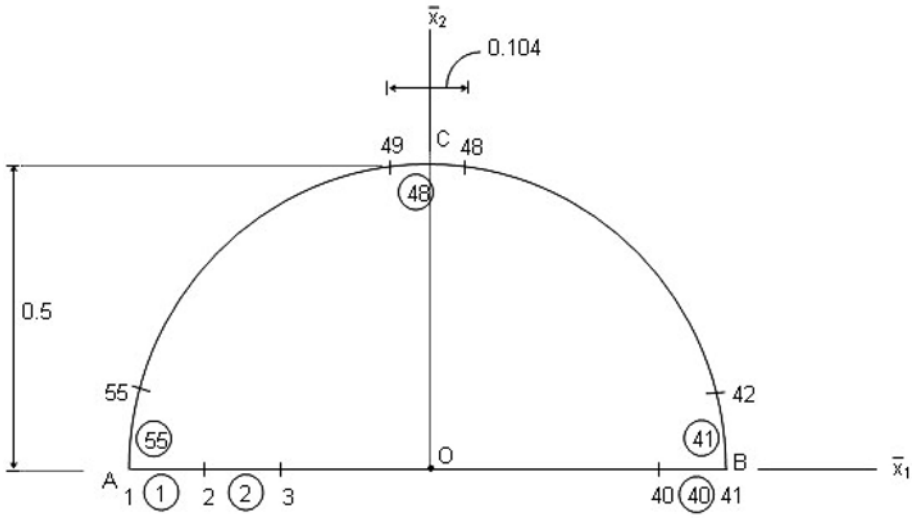

Fig. 7 Network used in circular disk problem

The exact distribution is computed by using

$$\tau_{22} = \frac{2p}{\pi d}\left[1 - \frac{4d^4}{(d^2 + 4x_1^2)^2}\right] \tag{33}$$

which is given in (Timoshenko and Goodier 1970). The Fig. 8 shows that discontinuous mixed BEM solutions compare very well with the exact, BEMLL and BEMQQ solutions. In this example, the BEMCC solution highly differs from the others especially at the end points of the region.

In Table 1, the type of the interpolation functions, the total numbers of boundary elements, boundary quantities and boundary unknowns used for alternative solution techniques are presented. It can be clearly seen from the table that, the use of BEMLC instead of BEMLL reduces the total number of unknown boundary quantities from 220 to 180, which means a drastic decline in the computing time, without reducing the accuracy of the solution. Similarly, the use of BEMQL

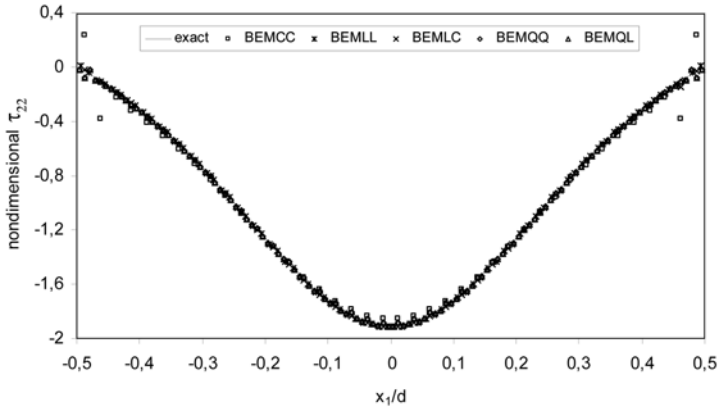

Fig. 8 The distribution of the stress component τ_{22} along the horizontal line AB

Table 1 Comparison of some parameters used in *Circular Disk Problem*

Software	Interpolation function for:		Total number of boundary elements	Total number of boundary quantities	Total number of boundary unknowns
	Displacement	Traction			
BEMCC	Constant	Constant	55	220	110
BEMLC	Linear	Constant	55	330	180
BEMLL	Linear	Linear	55	440	220
BEMQL	Quadratic	Linear	55	550	290
BEMQQ	Quadratic	Quadratic	55	660	330

instead of BEMQQ reduces the number of unknown boundary quantities significantly.

4.2 Rigid strip on a half space

A rigid strip of width $2b$ welded to the top surface of a half space is considered (see, Fig. 9). The half space is made of an isotropic elastic material. The rigid strip is under the influence of a vertical uniform line load P along x_3 axis. The parts (B) of the top surface outside the strip foundation are free of tractions. Here, the vertical stress distribution underneath the foundation is investigated.

This plane strain problem is solved by using the software BEMLC and BEMQL. The network used in BEM analysis is shown in Fig. 10. The upper boundary is truncated at the points C and D. The region CA, AB and BD are subdivided into 80, 40 and 80 subsegments respectively. Total number of elements is 200. The following non-dimensional variables and parameters are used in the analysis

$$\overline{x}_i = \frac{x_i}{b}; \quad \overline{u}_i = \frac{u_i}{b}; \quad \overline{t}_i = \frac{t_i}{\mu} \quad (i = 1,2)$$

$$\overline{p} = \frac{p}{\mu b}; \quad \overline{\mu} = \frac{\mu}{\mu} = 1; \quad \overline{\tau}_{22} = \frac{\tau_{22} b}{p}; \quad \overline{b} = \frac{b}{b} = 1 \tag{34}$$

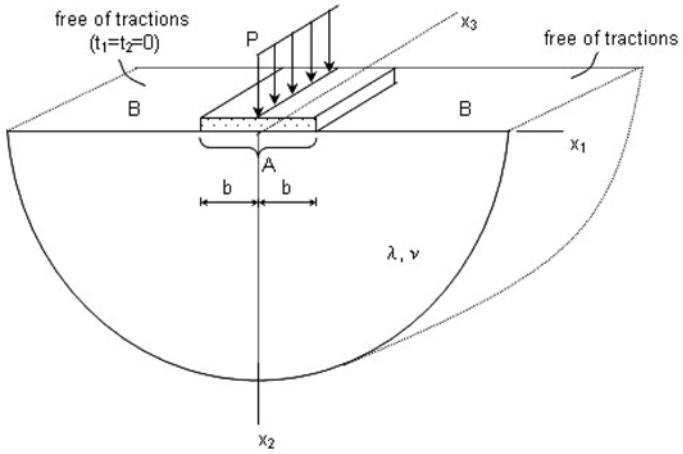

Fig. 9 Rigid strip on a half space

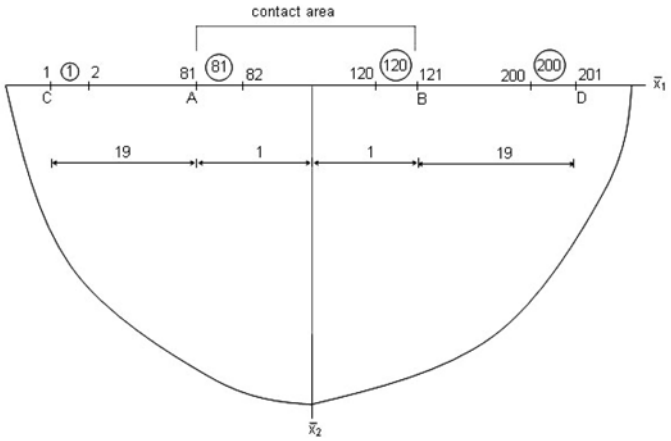

Fig. 10 Network used in rigid strip problem

In the computations, Poisson's ratio is taken as $\nu = 0.25$.

Our object in this problem is to obtain the vertical stress distribution underneath the foundation by discontinuous mixed BEM (BEMLC and BEMQL) and compare it with the results obtained by the BEMCC (Mengi *et al.* 1994), BEMLL (Severcan 2004), BEMQQ (Severcan 2004) and with the exact one given in (Saada 1974) as

$$\tau_{22} = -\frac{P}{\pi\sqrt{b^2 - x_1^2}} \tag{35}$$

The boundary conditions for the top surface of the half space are as follows

$$\begin{aligned} &\bar{u}_1 = 0;\ \bar{u}_2 = 1 \quad \text{on A (the region underneath the foundation)} \\ &\bar{t}_1 = 0;\ \bar{t}_2 = 0 \quad \text{on B} \end{aligned} \tag{36}$$

The distribution of stress component τ_{22} along the line AB obtained by discontinuous mixed BEM

is presented and compared with the exact one and with the results obtained by BEMCC, BEMLL and BEMQQ solutions in Fig. 11.

The type of the interpolation functions, the total numbers of boundary elements, boundary quantities and boundary unknowns used for alternative solution techniques in this problem are presented in Table 2. Again, it can be seen from the table that, the use of BEMLC and BEMQL instead of BEMLL and BEMQQ reduces the number of unknown boundary quantities significantly.

4.3 Infinite plate with a circular hole

In this example, considering that a plate of horizontal length $L_1 = 20$ m. and vertical length $L_2 = \infty$ containing a circular hole of radius $a = 1$ m and subjected to a uniaxial tensile stress σ_0 as seen in Fig. 12.

Because of symmetry conditions, only a quarter of the plate is considered and modeled as shown in Fig. 13. Due to the vertical length $L_2 = \infty$, there is no element at the boundary EF as seen in Fig. 13. Note that small elements are placed in the region of expected rapid variation of stresses around the hole. Here, the tangential stress σ_θ along the vertical line GA is investigated.

This plane stress problem is analyzed by using the softwares BEMLC and BEMQL. In the analysis, Poisson's ratio, Elasticity module and tensile stress are taken as $\nu = 0.3$, $E = 1$ N/m^2, $\sigma_0 = 1$ N/m^2, respectively.

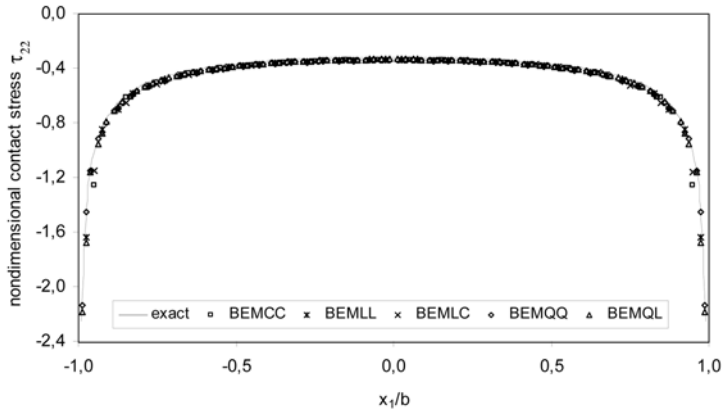

Fig. 11 The distribution of the stress component τ_{22} along the contact boundary AB

Table 2 Comparison of some parameters used in *Rigid Strip On a Half Space*

Software	Interpolation function for:		Total number of boundary elements	Total number of boundary quantities	Total number of boundary unknowns
	Displacement	Traction			
BEMCC	Constant	Constant	200	800	400
BEMLC	Linear	Constant	200	1200	720
BEMLL	Linear	Linear	200	1600	800
BEMQL	Quadratic	Linear	200	2000	1120
BEMQQ	Quadratic	Quadratic	200	2400	1200

The distribution of tangential stress σ_θ along the vertical line GA around circular hole in an infinite plate obtained BEMLC and BEMQL is compared with the results obtained by the BEMCC (Mengi *et al*. 1994), BEMLL (Severcan 2004), BEMQQ (Severcan 2004) and the analytical solution in Fig. 14. The analytical solution for the tangential stress around a hole in an infinite plate is computed by using

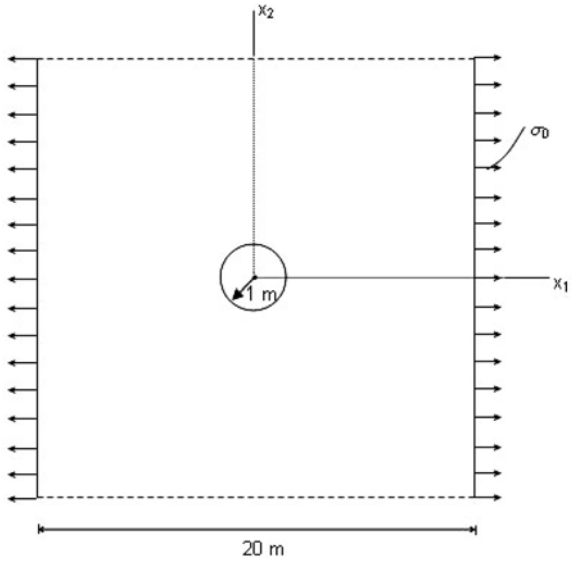

Fig. 12 Infinite plate with a circular hole subjected to a uniaxial tensile stress

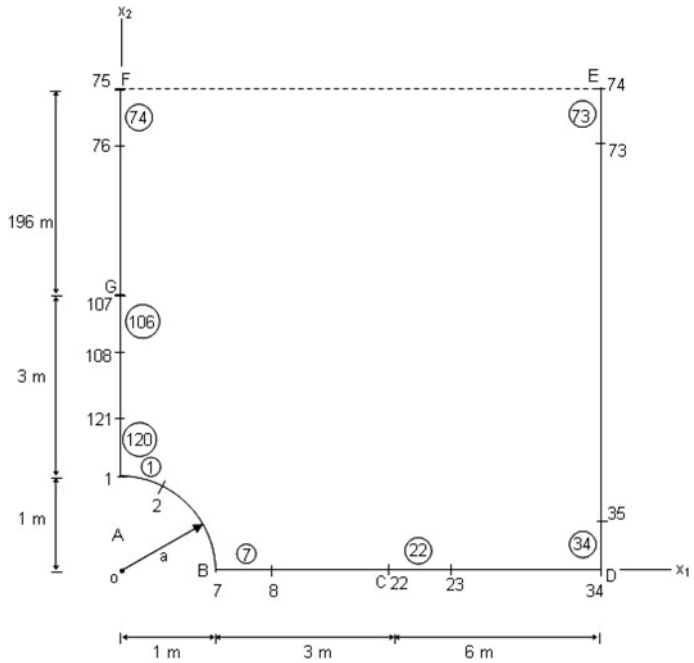

Fig. 13 Network used in circular hole problem

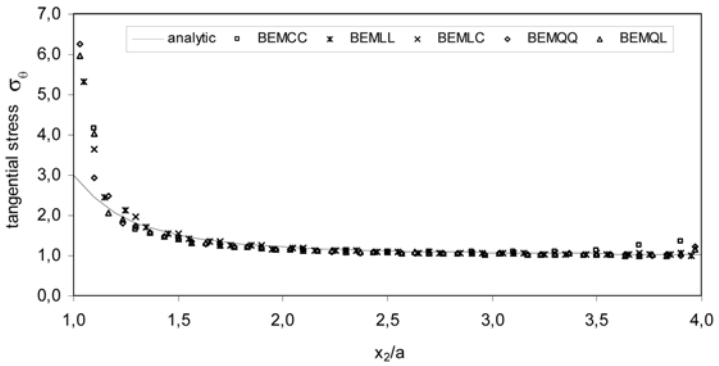

Fig. 14 The distribution of tangential stress σ_θ along the vertical line GA

Table 3 Comparison of some parameters used in *Infinite Plate with a Circular Hole*

Software	Interpolation function for:		Total number of boundary elements	Total number of boundary quantities	Total number of boundary unknowns
	Displacement	Traction			
BEMCC	Constant	Constant	120	480	240
BEMLC	Linear	Constant	120	720	406
BEMLL	Linear	Linear	120	960	480
BEMQL	Quadratic	Linear	120	1200	646
BEMQQ	Quadratic	Quadratic	120	1440	720

$$\sigma_\theta = \frac{\sigma_0}{2}\left(2 + \frac{a^2}{r^2} + 3\frac{a^4}{r^4}\right) \tag{37}$$

which is given in (Timoshenko and Goodier 1970). Here, a is the radius of the circular hole and r is the distance from the centre of the hole. The Fig. 14. shows that discontinuous mixed BEM solution compares very well with the exact one, however, in the light of the results numerous run over various mesh, although, discontinuous mixed BEM solutions are unexpectedly unusual around the hole and at the end points of the region in which stress varies rapidly, on the other hand, BEMLC and BEMQL solutions are slightly better approached to the exact one compared with the BEMCC, BEMLL and BEMQQ solutions.

Here, we compare the type of the interpolation functions, the total numbers of boundary elements, boundary quantities and boundary unknowns used for alternative solution techniques once again in Table 3, to highlight the advantages of the use of BEMLC and BEMQL instead of BEMLL and BEMQQ.

5. Conclusions

In this study, two discontinuous mixed boundary element formulations for 2D elastostatic problems are presented. The formulations are performed by using discontinuous first-order and

second-order mixed boundary elements. Based on these formulations, general purpose computer softwares (BEMLC and BEMQL) are developed and they are applied to 2D elastostatic problems.

The formulations and the computer softwares developed in this study are assessed by applying them to three example problems. The results are compared with those obtained by exact ones and the results obtained by constant BEM, discontinuous pure linear and discontinuous pure quadratic BEM solutions. The comparisons indicated that, the use of the mixed boundary element formulation diminishes the number of boundary unknowns without any reduction in the accuracy of the solution. This advantage will probably be more important in the elastostatic analysis of the problem having a complex geometry required an intensive meshing on the boundary. Hence, the formulations and the softwares developed in this study could be used with a good confidence in the elastostatic analysis of 2D problems.

References

Banerjee, P.K. (1994), *The Boundary Element Methods in Engineering,* McGraw-Hill Book Company, London.

Becker, A.A. (1992), *The Boundary Element Method in Engineering,* McGraw-Hill Book Company, London.

Brebbia, C.A. and Dominguez, J. (1989), *Boundary Elements an Introductory Course,* Computational Mechanics Publications, Southampton.

Dyka, C.T. and Millwater, H.R. (1989), "Formulation and integration of continuous and discontinuous quadratic boundary elements for two dimensional potential and elastostatics", *Comput. Struct.*, **31**(4), 495-504.

Liu, Y., Zhang, D. and Rizzo, F.J. (1993), "Nearly singular and hypersingular integrals in the boundary element method", *Boundary Elements XV, Proceedings of the 15th International Conference on Boundary Elements*, Worcester.

Manolis, G.D. and Beskos, D.E. (1987), *Boundary Element Method in Elastodynamics,* Unwin Hyman, London.

Mengi, Y., Tanrıkulu, A.H. and Tanrıkulu, A.K. (1994), *Boundary Element Method for Elastic Media, an Introduction,* METU Pres, Ankara.

Saada, A.S. (1974), *Elasticity Theory and Applications,* Pergamon Press Inc., New York.

Severcan, M.H. (2004), *Boundary Element Method Formulation for Dynamic Soil-structure Interaction Problems,* Ph.D. Dissertation (in Turkish), University of Cukurova, Turkey.

Sladek, V. and Sladek, J. (1998), "Singular integrals and boundary elements", *Comput. Method Appl. M.,* **157**, 251-266.

Sladek, V., Sladek, J. and Tanaka, M. (2001), "Numerical integration of logarithmic and nearly logarithmic singularity in BEMs", *Appl. Math. Model.*, **25**, 901-922.

Timoshenko, S. and Goodier, J.N. (1970), *Theory of Elasticity*, McGraw-Hill, New York.

Zhang, X.S. and Zhang, X.X. (2003), "Exact integration in the boundary element method for two-dimensional elastostatic problems", *Eng. Anal. Bound. Elem.,* **27**, 987-997.